Modern Solar Facilities – Advanced Solar Science, 1–4
F. Kneer, K. G. Puschmann, A. D. Wittmann (eds.)

Structure and evolution of supergranulation from local helioseismology

J. Hirzberger[1,*], L. Gizon[1], S. K. Solanki[1], and T. L. Duvall, Jr.[2]

[1]Max-Planck-Institut für Sonnensystemforschung, Katlenburg-Lindau, Germany
[2]Laboratory for Astronomy and Solar Physics, NASA/GSFC, Greenbelt,USA
[*]*Email:* hirzberger@mps.mpg.de

Abstract. Maps of the horizontal divergence of the near-surface velocity field have been calculated using local helioseismology and SOHO/MDI full-disk Dopplergrams. These maps provide a continuous coverage for two to three months each year with a cadence of 12 hours. Geometrical and evolutional properties of individual supergranular cells have been studied. Supergranular cells have sizes in a range around 650 Mm^2 (circular diameter of 28.77 Mm) with lifetimes of up to 4.5 days. We also observe a clear trend for larger cells to have stronger divergence values and larger lifetimes than smaller ones.

1 Data

The basic data used for this study are time series of full-disk Dopplergrams of several months length, obtained in a period between 1996 and 2002 with the Michelson Doppler Imager onboard the SOHO spacecraft. To extract information about supergranular flows the techniques of f-mode time-distance helioseismology (see Duvall & Gizon 2000) have been applied. The resulting data consist of 120°×120° (heliographic coordinates) divergence maps of the horizontal flow field ($\nabla \cdot \boldsymbol{v}_\mathrm{h}$) in a depth of 1 Mm below the solar surface (see Fig. 1). The spatial sampling rate of these maps amounts to 0.24° and the cadence is 12 h. The maps are interpolated onto a longitude-latitude (ϕ-λ) grid and structures with sizes $l > 250$ (<17.49 Mm) are filtered out. Since the noise levels in the divergence maps increases with distance from disk center only regions within a radius of 48° have been considered in the subsequent statistical analysis.

2 Image segmentation

Individual supergranular structures are detected by applying a segmentation algorithm to the divergence maps based on band-pass filtering in the Fourier domain (see Roudier & Muller 1987). The obtained structures are related to regions of strong positive divergence values which are the central regions of supergranular cells. In order to capture the entire dimensions of the supergranular cells local divergence minima have been searched. These are pixels for which all surrounding pixels have higher values. Then each detected supergranular structure has been dilated against the surrounding local minima. Hence, the FOVs are fully covered by the thus obtained supergranular cells.

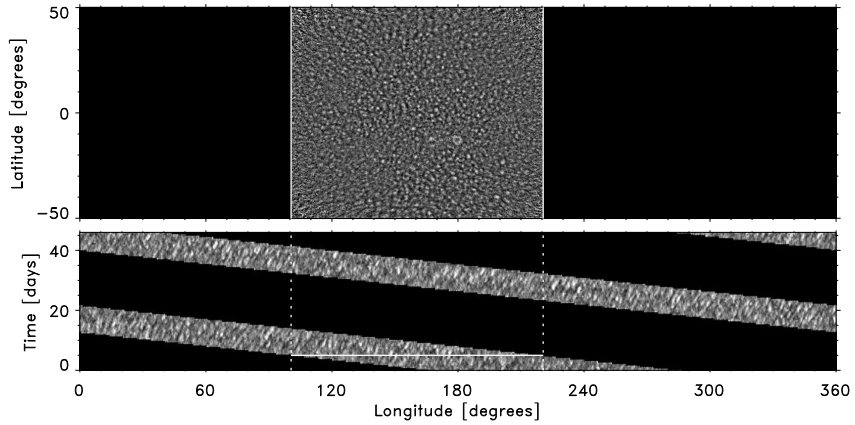

Figure 1. Time series of divergence maps obtained with f-mode time-distance helioseismology techniques. The upper panel shows a single map from the series. Light structures are regions where $\nabla \cdot \boldsymbol{v}_\mathrm{h} > 0$ (supergranules); in dark regions is $\nabla \cdot \boldsymbol{v}_\mathrm{h} < 0$ (inter-supergranular lanes). In the lower panel an x-t-slice of the series from the year 2000 is displayed. At all times only one third (120°) of the entire solar longitude range is visible.

Alternatively, the Fourier-based segmentation algorithm has been also applied to structures of strong convergence ($\nabla \cdot \boldsymbol{v}_\mathrm{h} < 0$). The thus obtained structures have larger areas and much more complex shapes which surround the divergence centers (see Fig. 2). Therefore, similar to "normal" solar granulation supergranulation defines a pattern of local divergence centers separated by a network of "inter-supergranular" lanes.

3 Cell structure

The distribution of detected supergranular cell areas (see Fig. 3) shows a well-defined maximum at $650\,\mathrm{Mm}^2$ (median value of distribution) which corresponds to a circular diameter of $d = \sqrt{4A/\pi} = 28.77\,\mathrm{Mm}$. The shape of the histogram is significantly different from that given in del Moro et al. (2004) who analyzed a much smaller statistical sample but have used similar data. However, it shows close similarity to distributions found by e.g. DeRosa & Toomre (2004). The mean divergence in most of the detected cells is close to zero which means that the supergranular cells are properly detected by the segmentation algorithm. The distribution of maximum divergences has a similar shape as the area histogram leading to an almost linear dependency between area and maximum divergence. Only the very largest cell structures seem to deviate from this correlation. Basically, this relation looks very similar to the area-intensity and area-velocity distributions found for "normal" granulation (see e.g. Hirzberger 2002). A close similarity in the structural properties of solar granulation and supergranulation was already stated in Berrilli et al. (2004).

4 Lifetimes

The time evolution of the supergranular cells has been studied by tracking the evolution of the segmented cells. The corresponding tracking algorithm is a modified version of the

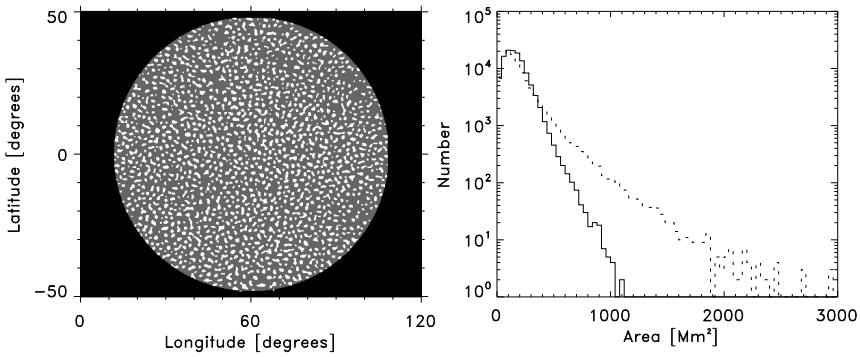

Figure 2. Fourier-based segmentation results. Left: Segmented divergence map; right: histograms of detected areas. The solid line shows the distribution of areas of divergence centers, the dotted line shows the distribution of convergence centers.

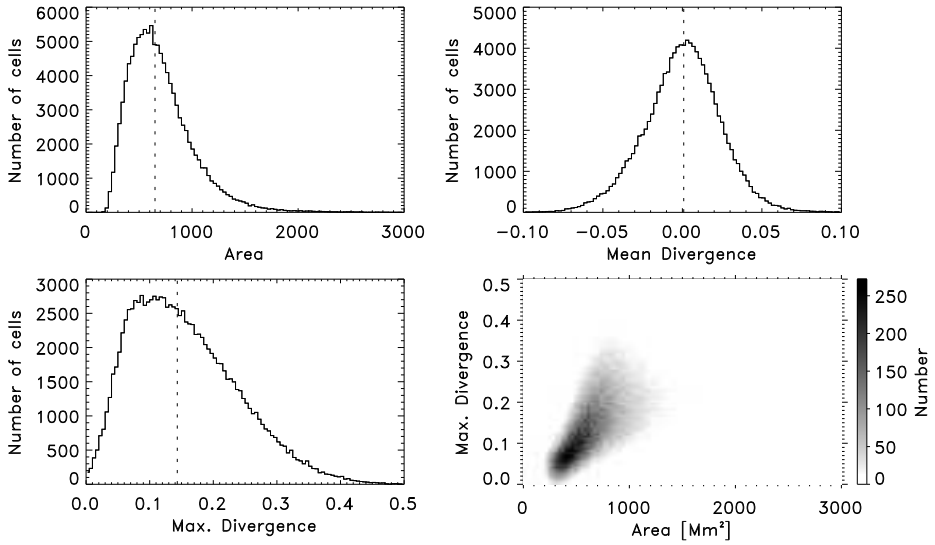

Figure 3. Histograms of areas, mean divergences, and maximum divergences of segmented supergranular cells. The vertical dotted lines represent median values of the distributions. The lower right panel shows a scatter plot of maximum divergence vs. cell area.

codes used for tracking granules (Hirzberger et al. 1999) and mesogranules (Leitzinger et al. 2005). Since the FOV is moving in longitude with time (see Fig. 1) only a small number of the detected supergranules can be followed from their "birth" to their "death". The thus estimated supergranular lifetimes and dynamical properties may be, therefore, biased by a selection effect. In addition, lifetimes below 12 hours are not resolved in the used data. The resulting lifetime histogram and variations of cell sizes and maximum divergences with supergranular lifetime is shown in Fig 5. Lifetimes up to 4.5 days have been detected although the bulk of supergranular cells have lifetimes between 1 and 3 days. Moreover, a tendency for longer-living structures to possess larger areas and stronger divergences can

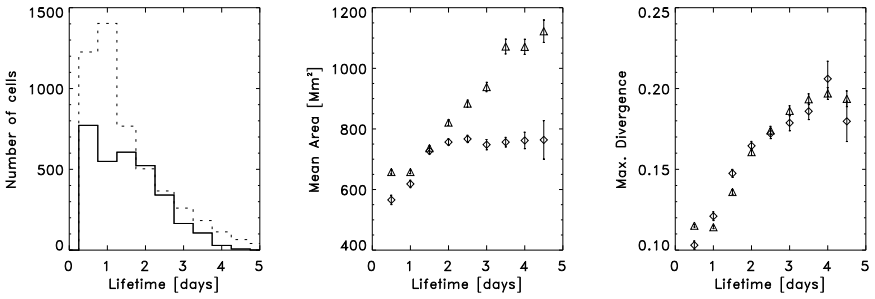

Figure 4. Evolutional parameters of supergranular cells: The left panel shows histograms of cell lifetimes (solid: feature tracking, dotted: 3d-segmentation). In the middle and right panels the time-averaged areas and maximum divergences of the lifetime histories have been once more averaged in each bin of the lifetime histograms (diamonds: feature tracking, triangles: 3d-segmentation). The error bars denote standard deviations of the mean ($\sigma/\sqrt{N}$) in each bin of the histogram.

be detected. This result is again in close similarity to the behavior of "normal" granulation cells.

As a second method to follow time evolution we applied a 3d-version of the Fourier segmentation algorithm mentioned above. The resulting structures represent supergranules in the ϕ-λ-t-space. These structures have been sliced for each time step and the thus recognized supergranules have also been dilated against the surrounding local divergence minima. The results of a subsequent statistical analysis are overplotted in Fig. 4.

5 Outlook

The fact that the data presented here cover a period between 1996 and 2002 establishes the possibility to study variations of supergranular structure and dynamics with the solar cycle. In addition, a possible dependence with solar latitude may be studied. Both topics require a careful analysis of magnetic field maps which are also available from the MDI data archive. If a such an extension of the data analysis would be successful important new insights into the interaction between solar magnetic fields and convection might be retrieved.

References

Berrilli, F., del Moro, D., Consolini, G., Pietropaolo, E., Duvall, T. L., Jr., & Kosovichev, A. G. 2004, Solar Phys., 221, 33
del Moro, D., Berrilli, F., Duvall, T. L., Jr., & Kosovichev, A. G. 2004, Solar Phys., 221, 23
DeRosa, M. L. & Toomre, J. 2004, ApJ, 616, 1242
Duvall, T. L., Jr. & Gizon, L. 2000, Solar Phys., 192, 177
Hirzberger, J. 2002, A&A, 392, 1105
Hirzberger, Bonet, J. A., Vázquez, M., & Hanslmeier, A. 1999, ApJ, 515, 441
Leitzinger, M., Brandt, P. N., Hanslmeier, A., Pötzi, W., & Hirzberger, J. 2005, A&A, 444, 245
Roudier, T. & Muller, R. 1987, Solar Phys., 107, 11